JOURNAL OF GEOPHYSICAL RESEARCH, VOL. 96, NO. D12, PAGES 22,559–22,572, DECEMBER 20, 1991

The Influence of Dynamics on Two-Dimensional Model Results: Simulations of ^{14}C and Stratospheric Aircraft NO_x Injections

CHARLES H. JACKMAN AND ANNE R. DOUGLASS

Laboratory for Atmospheres, NASA Goddard Space Flight Center, Greenbelt, Maryland

KURT F. BRUESKE

Research and Data Systems Corporation, Greenbelt, Maryland

STEPHEN A. KLEIN

Department of Atmospheric Science, Seattle, Washington

A two-dimensional (2D) photochemical model (latitude range from −85° to +85° and altitude range from the ground to 0.23 mbar (about 60 km)) has been used to investigate the influence of dynamics on model results. We tested three representations of atmospheric transport to simulate total ozone and ^{14}C amounts after nuclear tests in the early 1960s. We also simulated three scenarios of NO_x injections from a proposed fleet of stratospheric aircraft and their effects on ozone. The three dynamical formulations used were Dynamics A, a base dynamics used in previous work with this model; Dynamics B, a strong circulation dynamics discussed by *Jackman et al.* [1989*a*]; and Dynamics C, the dynamics used by *Shia et al.* [1989]. The advective component of the stratosphere to troposphere mass exchange rate (advective strat/trop exchange rate (ASTER)) is largest for Dynamics B (5.8×10^{17} kg yr^{-1}) and smallest for Dynamics C (1.4×10^{17} kg yr^{-1}), with the ASTER for Dynamics A (2.4×10^{17} kg yr^{-1}) being between these two extremes. Simulations of both total ozone and ^{14}C were worst with Dynamics B. Simulations of total ozone were best with Dynamics A and for ^{14}C best with Dynamics C. This illustrates the difficulty of simultaneously modeling constituents with different altitude and latitude dependencies. Ozone depletion from NO_x injections of stratospheric aircraft showed a strong sensitivity to dynamics. Generally, if eddy diffusion is not changed, then a large ASTER leads to reduced ozone loss while a small ASTER leads to increased ozone loss from a given stratospheric NO_x injection.

1. INTRODUCTION

Two-dimensional (2D) models are used extensively to study the middle atmosphere. These 2D models, while particularly suitable for assessment studies [World Meteorological Organization (*WMO*), 1990], are also used in a variety of other applications to understand atmospheric behavior [e.g., *Garcia et al.*, 1984; *Russell et al.*, 1984; *Ko et al.*, 1986; *Tung and Yang*, 1988; *Gray and Pyle*, 1989; *Legrand et al.*, 1989; *Jackman et al.*, 1991]. Measurements of some species are especially useful to check the photochemistry of 2D models (e.g., OH and HO_2) while measurements of other species (e.g., $CFCl_3$ and N_2O) are more useful to check the transport (advection and diffusion) of 2D models. Many stratospheric constituents are controlled by both transport and photochemistry, thus if there is a disagreement between model and measurement, it is often very difficult to decide which model aspect (transport or photochemistry) is in error.

Stratospheric 2D models are used primarily to assess and predict total ozone levels in the atmosphere. A major requirement of these models therefore is a good simulation of total ozone. Several 2D models have achieved a reasonably good qualitative representation of the total ozone seasonal behavior when compared to total ozone measurements [e.g., *Pyle*, 1980; *Garcia and Solomon*, 1983; *Ko et al.*, 1984; *Stordal et al.*, 1985; *Jackman et al.*, 1989*a*, *b*; *Yang et al.*, 1991]. While a reasonable simulation of present-day total ozone amounts is a required condition of 2D models, good simulations of ozone do not necessarily imply good simulations of other atmospheric constituents.

Other atmospheric constituents which provide checks on the model dynamics include inert tracers. The radioactive isotope ^{14}C has a half-life of 5730 years [*Warneck*, 1988, p. 573]. Although recent observational [*Tans et al.*, 1990] and modeling [*Shia et al.*, 1989] evidence has cast doubt on the relative importance of the oceans as a loss of carbon (relative to the continents), we have assumed that the oceans are the only significant means for surface loss of carbon and hence ^{14}C. Carbon 14 is rapidly converted to $^{14}CO_2$ which is photochemically inactive in the troposphere and stratosphere.

The remainder of this paper is divided into seven sections. We discuss the atmospheric model employed in our research and the three dynamical formulations in section 2. Comparison of model simulations of total ozone for the three dynamical formulations with total ozone mapping spectrometer (TOMS) measurements are given in section 3. Baseline model simulations of ^{14}C for a nonperturbed atmosphere are discussed in section 4. We present model predictions of the time-decay of ^{14}C amounts from nuclear explosions in the early 1960s in section 5. Model assessments for the change in ozone assuming NO_x injections by stratospheric aircraft are

Paper number 91JD02510.
0148-0227/91/91JD-02510$05.00

TABLE 1. Lower Boundary Conditions for All Transported Species in Total Ozone Simulations Given in Figure 1 and for Cl_x Perturbations Discussed

Species	Type of Boundary Condition, Units	1980 Value, $Cl_x \approx 2.5$ ppbv	Perturbed Value, $Cl_x \approx 8.2$ ppbv
N_2O	mixing ratio, ppbv	300	360
CH_4	mixing ratio, ppmv	1.6	3.2
CO	mixing ratio, ppbv	100	100
H_2	mixing ratio, ppbv	500	500
CH_3OOH	flux, $cm^{-2}\ s^{-1}$	0.0	0.0
CH_3Cl	mixing ratio, pptv	700	700
CH_3CCl_3	mixing ratio, pptv	100	100
CCl_4	mixing ratio, pptv	100	100
$CFCl_3$	mixing ratio, pptv	170	800
CF_2Cl_2	mixing ratio, pptv	285	2200
O_x	deposition velocity, $cm\ s^{-1}$	0.1	0.1
HNO_3	mixing ratio, pptv	90	90
NO_y(wo HNO_3)	mixing ratio, pptv	10	10
Cl_x	flux, $cm^{-2}\ s^{-1}$	0.0	0.0

Units are in parts per billion by volume (ppbv), parts per million by volume (ppmv), and parts per trillion by volume (pptv).

given in section 6, while discussion and conclusions are presented in section 7.

2. Model Description and Dynamical Formulation

The 2D model used in this study is described by *Douglass et al.* [1989] and applied in an assessment of the atmosphere for a chlorine perturbation in *Jackman et al.* [1989*a*]. The model vertical coordinate is between the ground and 0.23 mbar (approximately 60 km), equally spaced in log pressure, with about a 2 km grid spacing, and the horizontal coordinate is from 85°S and 85°N with a 10° grid spacing. The lower boundary conditions for the year 1980 are given in Table 1 for the model background: ≈2.5 parts per billion per volume (ppbv) Cl_x input at the ground. Simulations of other years include different lower boundary conditions and will be discussed below. The upper boundary conditions were assumed to be zero flux for all species. Reaction rates and photodissociation cross sections are taken from *DeMore et al.* [1987] and given by *Douglass et al.* [1989].

Three different dynamical formulations, Dynamics A, B, and C, were used in the model calculations. Both Dynamics A and B are described and applied to a chlorine perturbation by *Jackman et al.* [1989*a*] and are referred to as the "combined circulation" and the "strong circulation," respectively. Dynamics C is described by *Shia et al.* [1989]. When used to simulate the behavior of ^{14}C, the three different dynamical formulations produce medium, large, and small advective mass exchange from the stratosphere to the troposphere.

The Dynamics A residual circulation is computed using heating rates and temperatures in the method formulated by *Dunkerton* [1978]. Heating rates are taken from *Rosenfield et al.* [1987] for pressures less than 100 mbar and from *Dopplick* [1974, 1979] for pressures from 100 mbar to the ground. Temperatures are defined from a 4-year average (1979–1983) of National Meteorological Center (NMC) data for pressures greater than 0.4 mbar and from COSPAR International Reference Atmosphere (CIRA) (1972) for pressures less than 0.4 mbar. The horizontal eddy diffusion coefficients (K_{yy}) were derived from the flux and gradient of potential vorticity using NMC temperatures [*Newman et al.*, 1988] from the same data set as the residual circulation. The smallest values allowed in the stratosphere are $2 \times 10^9\ cm^2\ s^{-1}$. The K_{yz} represent the ratio of the mixing on isentropic surfaces to the mixing on pressure surfaces and are computed from the K_{yy} values and the potential temperature [*Newman et al.*, 1988; *Jackman et al.*, 1988]. The K_{yy} values in the troposphere are tapered up to the largest values of $2 \times 10^{10}\ cm^2\ s^{-1}$ at the ground. The vertical eddy diffusion K_{zz} is assumed to be small in the stratosphere ($2 \times 10^3\ cm^2\ s^{-1}$), increasing with decreasing altitude from the tropopause to $1 \times 10^5\ cm^2\ s^{-1}$ at the ground.

The Dynamics B residual circulation is also computed from heating rates and temperatures in the method formulated by *Dunkerton* [1978]. Heating rates are taken from *Rosenfield et al.* [1987] for pressures less than 100 mbar and from *Wei et al.* [1983] for pressures from 100 mbar to the ground. The temperatures and eddy diffusion parameters K_{yy}, K_{yz}, and K_{zz} are the same as discussed above for Dynamics A. Thus this transport differs from Dynamics A only in the residual circulation between the ground and 100 mbar.

The residual circulation and diffusion for Dynamics C is taken from *Shia et al.* [1989]. The transport coefficients are originally given by *Yang et al.* [1990] for their isentropic 2D model. Yang et al. computed the diabatic circulation from the NMC 1980 temperature field and self-consistently determined the isentropic diffusion coefficients by solving the momentum equation. Shia et al. have converted this isentropically derived transport formulation to a 2D model with a pressure grid. Shia et al. have also specified K_{yy} in the troposphere as $1 \times 10^{10}\ cm^2\ s^{-1}$ and have fixed stratospheric K_{zz} at $1 \times 10^2\ cm^2\ s^{-1}$ and tropospheric K_{zz} as $1 \times 10^5\ cm^2\ s^{-1}$.

Dynamics C has a circulation grossly similar in many respects to the circulation of Dynamics A. There are, however, subtle but important differences in the magnitude of the vertical and meridional winds. The stratospheric vertical and horizontal diffusion are quite different between Dynamics C and those used in Dynamics A and B. Vertical diffusion (K_{zz}) in Dynamics C is lower than that in Dynamics A and B by a factor of 20. The K_{yy} in Dynamics C have a

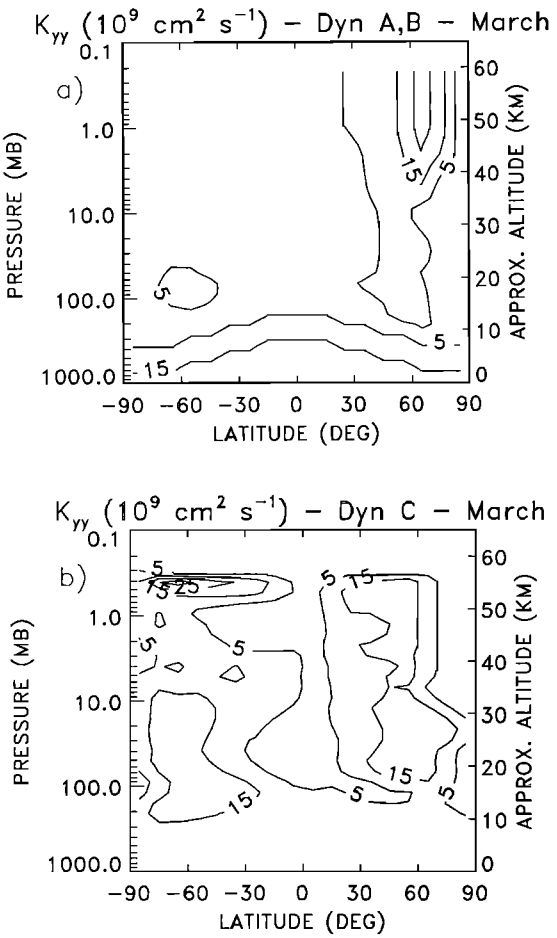

Fig. 1. Horizontal eddy diffusion (K_{yy}) in units of 10^9 cm^2 s^{-1} from (*a*) Dynamics A–B and (*b*) Dynamics C for March. Contour intervals are 5, 15, 25, and 35.

different lower limit (1×10^8 cm^2 s^{-1} in Dynamics C versus 2×10^9 cm^2 s^{-1} in A and B) as well as a different altitude and latitude structure from those given in Dynamics A and B.

The tropospheric K_{yy} and K_{zz} levels are also different for Dynamics C compared with those of Dynamics A and B. Dynamics A and B have K_{yy} and K_{zz} values that taper from the tropopause to large values in the lower troposphere, whereas Dynamics C shows a sharp discontinuity at the tropopause, ranging from small stratospheric levels to large tropospheric values over one grid box. Tropopause heights in Dynamics A and B compared with Dynamics C, while mostly the same, do show one grid box differences at certain latitudes and seasons.

As an illustration of the differences between the different dynamical representations, we plot K_{yy} for the month of March from Dynamics A–B and C in Figures 1*a* and 1*b*, respectively. Fairly large differences as functions of latitude and altitude are obvious when comparing the two dynamical representations. It is impossible to discuss completely all the dynamical differences in Dynamics A, B, and C. We do, however, summarize the references used to represent the three dynamical formulations as well as some relevant values of eddy diffusion in Table 2.

In a time-averaged global domain the residual circulation can be used to provide at least a crude estimate of the mass exchange between the stratosphere and the troposphere. Consider a stratospheric volume bounded below by the tropopause, above by the 50 mbar surface, and extending from 30° to 90°N. The vertical mass flux through the tropopause, F_{trop}, is calculated according to

$$F_{trop} = 2\pi r_e^2 \int_{30°N}^{90°N} \rho_0 w^* \cos\phi \, d\phi$$

where r_e is the radius of the Earth, ρ_0 is the density, and w^* is the residual vertical velocity across the tropopause. There are uncertainties in this computation of the mass exchange, two of which are (1) an uncertainty inherent in a residual advection representation of the mean motions of the atmosphere and (2) the uncertainty associated with the computations of the heating rates in the lower stratosphere which are then used to compute the residual circulation. Since 2D models, based on the residual circulation formulation, have been relatively successful in representing stratospheric constituents (see discussion in section 1), we consider use of our residual circulation 2D model to be a reasonable method of studying problems related to the lower stratosphere.

The value of F_{trop} is computed to be 2.4×10^{17} kg yr^{-1} for Dynamics A, 5.8×10^{17} kg yr^{-1} for Dynamics B, and 1.4×10^{17} kg yr^{-1} for Dynamics C. Smaller values of F_{trop} imply longer residence times for constituents in the lower stratosphere, whereas larger values of F_{trop} imply the converse. These may be compared with the estimate of *Holton* [1990] for the mass flux through the 100 mbar surface of 1.3×10^{17} kg yr^{-1} and a minimum estimate of 1×10^{17} kg yr^{-1} given by *Robinson* [1980]. Clearly, the advective component of the

TABLE 2. Summary of Different Dynamical Formulations Applied

	Dynamics Formulation		
	A, Base	B, Strong	C, *Shia et al.* [1989]
Temperature	NMC (1979–1983)	NMC (1979–1983)	NMC (1980)
Q, $P < 100$ mbar	*Rosenfield et al.* [1987]	*Rosenfield et al.* [1987]	*Yang et al.* [1990]
Q, $P > 100$ mbar	*Dopplick* [1974, 1979]	*Wei et al.* [1983]	*Yang et al.* [1990]
Advection	Residual circulation *Jackman et al.* [1989*a*]	Residual circulation *Jackman et al.* [1989*a*]	Diabatic circulation *Yang et al.* [1990]
Stratospheric K_{yy}	*Newman et al.* [1988]	*Newman et al.* [1988]	Derived from diabatic circulation
Stratospheric K_{zz}	2×10^3 cm^2 s^{-1}	2×10^3 cm^2 s^{-1}	1×10^2 cm^2 s^{-1}
Tropospheric K_{yy}	tapered to 2×10^{10} cm^2 s^{-1}	tapered to 2×10^{10} cm^2 s^{-1}	1×10^{10} cm^2 s^{-1}
Tropospheric K_{zz}	tapered to 1×10^5 cm^2 s^{-1}	tapered to 1×10^5 cm^2 s^{-1}	1×10^5 cm^2 s^{-1}

NMC is National Meteorological Center.

stratosphere to troposphere mass exchange rate (advective strat/trop exchange rate (ASTER)) for Dynamics C is closest to the estimate of Holton, with the ASTER for Dynamics A being within a factor of 2 of the Holton estimate. The extremely large ASTER for Dynamics B is probably outside the bounds of what might be considered possible for the atmosphere.

3. Total Ozone Simulations

Measurements from ground-based instruments and satellite measurements over a period of many years provide a good global climatology of total ozone. The TOMS instrument on Nimbus 7 has measured global total ozone since 1979 and provides a consistent set of measurements for over a decade. No other stratospheric constituent has been monitored to such an extent.

Most stratospheric modeling efforts revolve around predictions and assessments of ozone [e.g., *WMO*, 1986, 1988, 1990] because of its importance in shielding living organisms from damaging ultraviolet (UV) radiation. Since ozone has been monitored so extensively and modeled so frequently, it is important that 2D model predictions of ozone be compared with measurements of ozone. The comparison between modeled and measured ozone gives some measure of the reliability of that particular model for predictions of ozone changes derived from increases in other trace gases in the atmosphere.

We use the three dynamical formulations in our model to predict total ozone for the year 1980 using lower boundary conditions given in Table 1. The total ozone over the course of a year as a function of latitude for the three separate model calculations and TOMS data for 1980 are given in Figure 2. TOMS data in Dobson units are shown in Figure 2*a* with Dynamics A, B, and C shown in Figures 2*b*, 2*c*, and 2*d*, respectively.

We compare our model results to three major features observed in TOMS data, namely, (1) an on-the-pole northern hemisphere late winter/early spring maximum; (2) equatorial ozone levels which follow the Sun with higher ozone in summer and lower ozone in winter; and (3) an off-the-pole southern hemisphere maximum in late winter/early spring which peaks around 60°S. The total ozone using Dynamics A shows good qualitative agreement with TOMS data for all three features compared (see Figures 2*a* and 2*b*). Differences between the model and measurement include (1) equatorial ozone is about 20 Dobson units (DU) higher than observed in TOMS data and (2) southern hemisphere on-the-pole ozone amounts are much lower in the TOMS data than predicted by the model.

The model prediction for total ozone using Dynamics B does not show as many similarities to TOMS data as those indicated above for a model simulation with Dynamics A (compare Figures 2*a*, 2*b*, and 2*c*). The first two major features noted in the TOMS data are simulated using Dynamics B in the model. Many differences are apparent between model and data including (1) equatorial ozone is about 20 DU lower than observed in TOMS data; (2) polar ozone is extremely large at both poles (>700 DU above 80°N for days 15–135), much greater than shown in TOMS data; and (3) the southern hemisphere off-the-pole maximum as observed in the TOMS data is not predicted by the model.

A model simulation with Dynamics C does a respectable

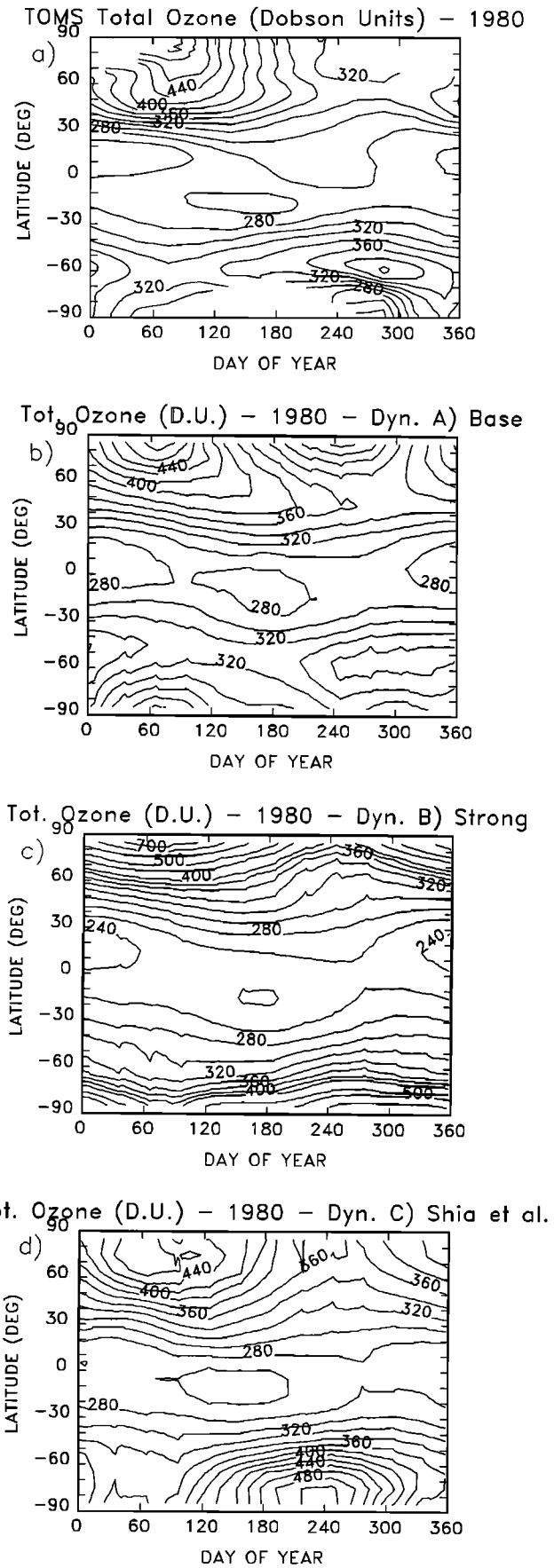

Fig. 2. Total ozone from (*a*) TOMS and model simulations with (*b*) Dynamics A, (*c*) Dynamics B, and (*d*) Dynamics C. Contour intervals are spacings of 20 Dobson units.

job of representing total ozone when compared with TOMS data (compare Figures 2*a* and 2*d*). The first two major features noted in the TOMS data are again simulated using Dynamics C in the model. Differences between the model and measurement include (1) the southern hemisphere off-the-pole maximum is not predicted by the model but is observed in the TOMS data and (2) southern hemisphere polar ozone amounts are much lower in the TOMS data than predicted by the model.

Model simulations using Dynamics A give a slightly better overall total ozone representation than model simulations using Dynamics C. Model simulations using the large AS-TER of Dynamics B show a poor representation of total ozone when compared to TOMS data.

4. Baseline Model Simulation of ^{14}C

Radioactive isotope ^{14}C is produced naturally by galactic cosmic rays but also can be injected into the atmosphere by nuclear explosions. Since ^{14}C appears in gaseous form (almost always as $^{14}CO_2$), it is thought to be quite suitable for use as a tracer [*List and Telegadas*, 1969; *Johnston et al.*, 1976; *Johnston*, 1989].

For the modeling of isotope ^{14}C, three physical processes (production, radioactive loss, and surface deposition velocity) need to be included. Radioactive loss is the simplest of these. The number of ^{14}C atoms lost per unit time is equal to λN_x, where $\lambda = \ln 2/\tau_{1/2}$, N_x is the number of ^{14}C atoms present, and $\tau_{1/2}$ is the half-life of ^{14}C. Production and surface deposition velocity are discussed in the ensuing paragraphs.

The natural continuous production of ^{14}C by galactic cosmic rays poses an uncertainty for modeling. High energy particles (of the order of MeV to GeV) react with N_2 and O_2 to form ^{14}C among other products. Most ^{14}C is produced near the poles where cosmic ray activity is most intense. Extensive direct measurements of the production do not exist; consequently, the calculated production rates have a large uncertainty. Two estimates of the global production rate of ^{14}C exist: 3.5×10^{26} atoms/yr [*Lingenfelter and Ramaty*, 1970] and 2.9×10^{26} atoms/yr [*Lal and Peters*, 1967]; however, latitude versus altitude profiles (in kilometers or millibars) of production rates are not in the literature to the best of our knowledge. Since ^{14}C is produced by cosmic rays, these profiles were assumed to be identical to those of radioactive isotope ^{7}Be [*Bhandari et al.*, 1966] scaled to give an annual production of 3×10^{26} atoms/yr.

The biosphere cycles its carbon content with the atmosphere on time scales of a few years; surface deposition processes are thought to be responsible for controlling the carbon cycle on much longer time scales. Until recently, it was believed [e.g., *Warneck*, 1988] that the long term abundance of ^{14}C in the atmosphere is determined by the loss of ^{14}C to the oceans whose carbon cycle time scale is of the order of thousands of years and comparable to the half-life of ^{14}C, 5730 years. At the ocean-air interface the amount of ^{14}C that enters the ocean is proportional to the amount in the atmosphere above the ocean, and the amount of ^{14}C that enters the atmosphere from the ocean is proportional to the amount of ^{14}C in the mixed layer of the ocean. On the basis of measurements of the actual amounts of natural ^{14}C in both the mixed layer of the ocean and the atmosphere, *Oeschger et al.* [1975] conclude that the flux of ^{14}C in and out of the ocean approximately cancel such that the net flux of ^{14}C at the ocean-air interface is only 0.05 ± 0.015 of the flux of ^{14}C into the ocean.

Recent studies (modeling by *Shia et al.* [1989] and data analysis by *Tans et al.* [1990]) have suggested that the continents may be responsible for the largest losses of CO_2 from the atmosphere. We have investigated this suggested land surface loss in a series of model sensitivity studies. Although we do not discuss these model experiments in any detail, we note that our computations of ^{14}C are in better agreement with observations when our surface loss is only dependent on the oceans. Furthermore, the stratospheric results are relatively insensitive to the boundary condition on time scales of our model simulations (a few years). We therefore only use the ocean component of surface loss in our model for ^{14}C.

Since our tropospheric dynamics is controlled by eddy diffusion (see Table 2), our model results should be used with caution when trying to address issues that may be dependent on the tropospheric dynamics. Our model simulations of ^{14}C do not support the continental carbon sink, however, we do not believe that our model computations necessarily refute the continental carbon sink either.

In our model the net loss of ^{14}C over oceans is included via a deposition velocity. The net change in concentration of ^{14}C per unit time in the lowest grid box of each latitude range is equal to $0.05\ (v_d/\Delta Z)c_n f_o$, where v_d is the deposition velocity, ΔZ is the height of the lowest box in our grid ($\approx$2 km), c_n is the concentration of ^{14}C in that box, and f_o is the fraction of the Earth's surface in that latitude bin covered by oceans.

The observed abundance of natural ^{14}C is 74×10^5 atoms/(gm air) or 3.57×10^{-16} in mixing ratio [*Telegadas*, 1971]. Because of its long half-life, ^{14}C is assumed to be uniformly mixed throughout the atmosphere. With a fixed input production rate (as given above) and the known abundance of natural ^{14}C, our 2D model can be used to calculate what deposition velocity is needed to maintain an atmosphere with a background ^{14}C of 74×10^5 atoms/(gm air). Thus our initial condition has 74×10^5 ^{14}C atoms/(gm air) everywhere in the atmosphere, and the model is integrated forward with a specific deposition velocity to see whether or not 74×10^5 ^{14}C atoms/(gm air) is maintained in the northern hemisphere troposphere. Most measurements of ^{14}C are in the northern hemisphere troposphere [*Telegadas*, 1971], thus model and measurements are compared in this region. Several runs with different deposition velocities were necessary to find the value of the deposition velocity that maintains this background level.

Our model indicates that the background ^{14}C is not uniformly mixed but varies by about 10% and is dependent on the local intensity of cosmic rays. To achieve a background abundance of 74×10^5 ^{14}C atoms/(gm air) in the northern hemisphere troposphere requires an ocean deposition velocity of 6.7×10^{-3} cm/s, a number in good agreement with the estimate of *Liss* [1988] of $5.6 \pm 1.4 \times 10^{-3}$ cm/s. The corresponding mean lifetime of ^{14}C atoms in the atmosphere being transferred to the mixed layer of the ocean (approximately equal to the mean lifetime of ^{12}C atoms or CO_2) is 6.2 years, in rough agreement with an average lifetime of 7 years derived from 12 other investigations [*Warneck*, 1988, p. 574].

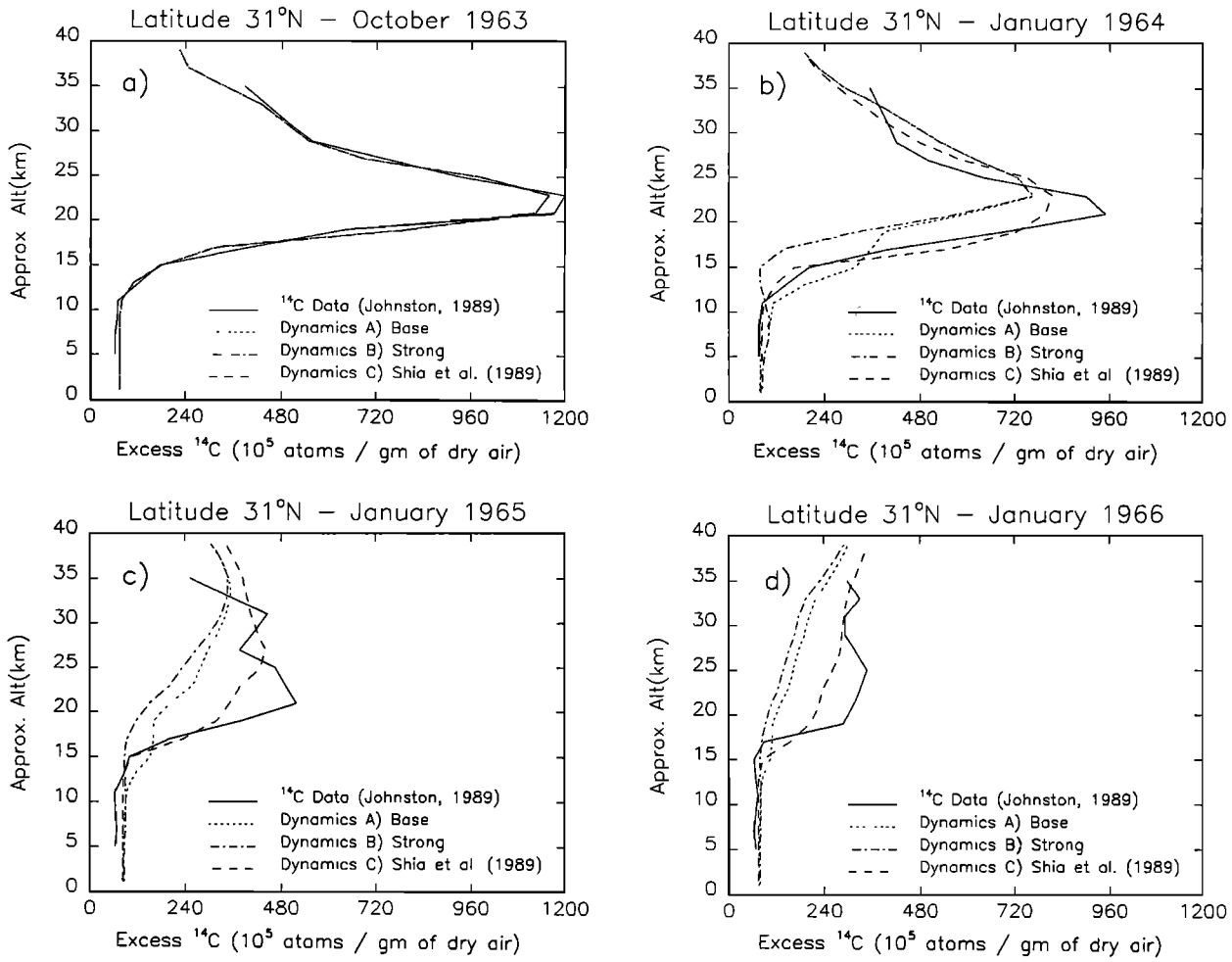

Fig. 3. Excess ^{14}C measurements and model simulations at 31°N at four different times: (*a*) October 1963, (*b*) January 1964, (*c*) January 1965, and (*d*) January 1966. Initial ^{14}C distribution in (*a*) for October 1963 (short dashed, dashed-dotted, and long dashed curves for the model simulations) is taken from *Johnston* [1989]. The solid curve represents the balloon data ((*a*), (*b*), (*c*), and (*d*)), while the short dashed, dashed-dotted, and long dashed curves represent the model simulation of ^{14}C for Dynamics A, B, and C, respectively, in (*b*), (*c*), and (*d*). The units are in 10^5 ^{14}C atoms per gram of dry air.

5. Model Simulations of ^{14}C Produced by Nuclear Explosions

Carbon 14 was produced in large quantities by every aboveground nuclear test carried out by the United States and the Soviet Union in the late 1950s and early 1960s. The concentration of ^{14}C was monitored by the Health and Safety Laboratory (HASL) program of the U.S. Atomic Energy Commission for several years during and after the testing period [*Telegadas*, 1968, 1971; *Telegadas and List*, 1969]. The subsequent decay in concentrations of ^{14}C provides a stringent test of 2D models. *Johnston* [1989] has recently advocated this test for ^{14}C and recently *Kinnison* [1989] and *Shia et al.* [1989] detailed their successful modeling of nuclear explosion-produced ^{14}C.

For studies of the lower stratosphere and upper troposphere, several gases (e.g., N_2O, CH_4, $CFCl_3$, CF_2Cl_2, HNO_3, O_3, and ^{14}C) have been employed as tracers to test the transport in models. There are properties of ^{14}C that make it particularly well suited to transport tests. All of these tracers have an atmospheric sink and/or source which can lead to problems in interpreting the agreement/disagreement between model and measurements. The loss of ^{14}C, while it resides in the atmosphere, by radioactive decay ($\tau_{1/2}$ = 5730 years) is fairly simple and small on a few-year time scale when compared to the losses of the other noted tracers. Therefore it is believed that if the starting amount of ^{14}C (in this case, excess ^{14}C, the ^{14}C produced by nuclear explosions) is known, then ^{14}C is one of the best tracers of motion in the atmosphere. Because it appears in gaseous form in the atmosphere, gravitational settling plays no role. Chemical models should be able to model the short term as well as the long term behavior of this tracer. Our test consists of trying to model the decay of the excess ^{14}C from October 1963 to January 1967. October 1963 is chosen because this month is six months after the last nuclear test, and thus ^{14}C was presumed to have achieved zonal symmetry. January 1967 is chosen as the cutoff date because this is immediately prior to the resumption of aboveground testing with the Chinese detonation of a 3 MT nuclear explosion in approximately April of 1967.

Carbon 14 data exist for four latitudes, 31°, 70°, and 9°N and 42°S. We compare model results to measurements for all these latitudes (see Figures 3, 4, 5, and 6).

Our initial conditions for October 1963 are taken from the

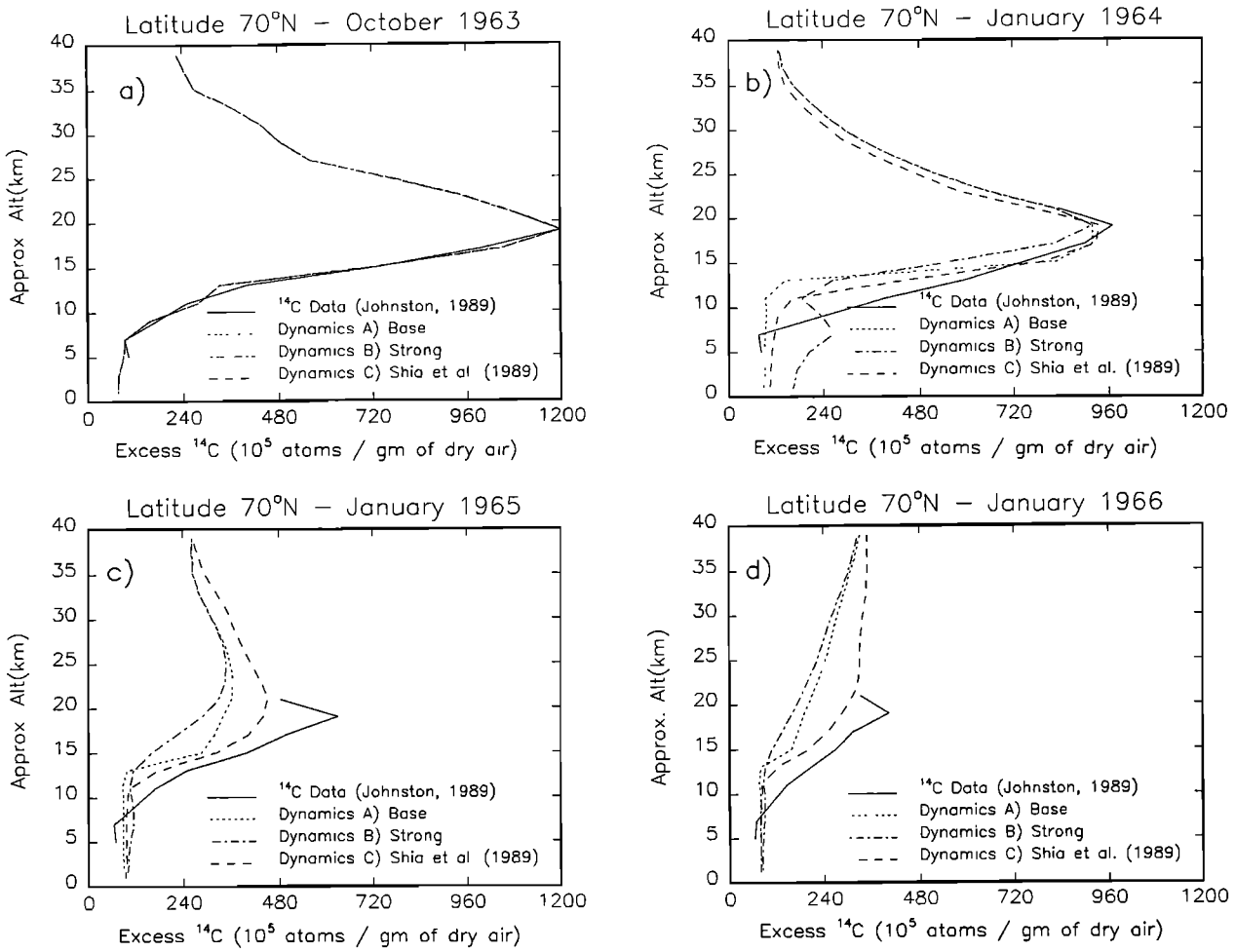

Fig. 4. Excess ^{14}C measurements and model simulations at 70°N at four different times: (*a*) October 1963, (*b*) January 1964, (*c*) January 1965, and (*d*) January 1966. Initial ^{14}C distribution in (*a*) for October 1963 (short dashed, dashed-dotted, and long dashed curves for the model simulations) is taken from *Johnston* [1989]. The solid curve represents the balloon data ((*a*), (*b*), (*c*), and (*d*)), while the short dashed, dashed-dotted, and long dashed curves represent the model simulation of ^{14}C for Dynamics A, B, and C, respectively, in (*b*), (*c*), and (*d*). The units are in 10^5 ^{14}C atoms per gram of dry air.

Johnston [1989] analysis of the experimental measurements for September to November of 1963 contained in *Telegadas* [1971]. These initial conditions (short dashed, dashed-dotted, and long dashed curves) are given in Figure 3*a* compared to measurements (solid curve). Because the greatest abundances of excess ^{14}C lie in the lower stratosphere at northern polar latitudes for October 1963 and most of the successive months, modeling of excess ^{14}C rigorously tests the dynamics of the lower stratosphere at northern middle to high latitudes.

We used the three dynamical formulations in modeling ^{14}C. In proceeding we integrated forward in time the total amount of ^{14}C (excess plus naturally occurring background ^{14}C), including the natural production, radioactive loss, and loss at the ocean-atmosphere interface. For the ocean-atmosphere interface our initial assumption was that the back flux of ^{14}C from the ocean did not increase and stayed at the level necessary to maintain the background ^{14}C. This assumption, while not strictly true since the back flux from the ocean certainly increased as the concentration of ^{14}C in the mixed layer of the ocean increased, is a reasonable one. For example, data from *Tans* [1981] indicate that the concentration of ^{14}C in the mixed layer of the ocean increased only 10% over background levels during this period; hence neglecting this increase in the back flux of ^{14}C from the ocean represents only a small error in the modeling. On short time scales, changes in the modeling of the troposphere have only a small effect on the modeling of the stratospheric abundances of excess ^{14}C.

Figures 3*b*, 3*c*, and 3*d* show model simulations and measurements of excess ^{14}C (above the background of 74 × 10^5 ^{14}C atoms/(gm air)) in January for the years 1964, 1965, and 1966, respectively. The Dynamics A simulation of ^{14}C gives a fairly reasonable representation of the tropospheric abundance of ^{14}C but seriously underestimates the abundance of ^{14}C in the lower stratosphere (see short dashed curve in Figures 3*b*, 3*c*, and 3*d*). The solid curve in Figure 3 shows this result for the balloon measurements of ^{14}C [*Johnston*, 1989].

Simulation of ^{14}C with Dynamics B (see dashed-dotted curve in Figures 3*b*, 3*c*, and 3*d*) is even worse in comparison to measurements than the simulation with Dynamics A. Carbon 14 is transported out of the stratosphere with Dy-

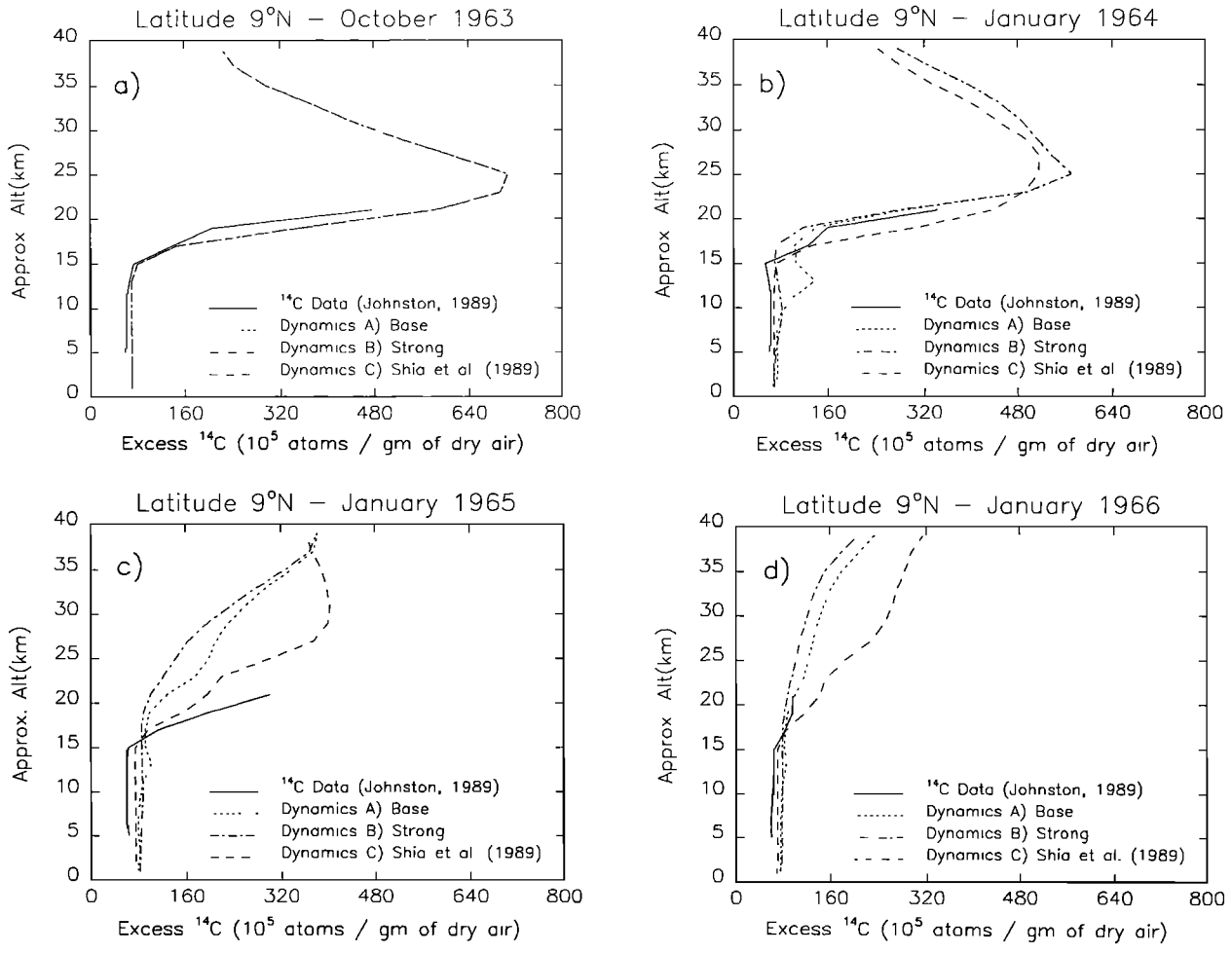

Fig. 5. Excess ^{14}C measurements and model simulations at 9°N at four different times: (*a*) October 1963, (*b*) January 1964, (*c*) January 1965, and (*d*) January 1966. Initial ^{14}C distribution in (*a*) for October 1963 (short dashed, dashed-dotted, and long dashed curves for the model simulations) is taken from *Johnston* [1989]. The solid curve represents the balloon data ((*a*), (*b*), (*c*), and (*d*)), while the short dashed, dashed-dotted, and long dashed lines represent the model simulation of ^{14}C for Dynamics A, B, and C, respectively, in (*b*), (*c*), and (*d*). The units are in 10^5 ^{14}C atoms per gram of dry air.

namics B much more quickly than indicated by the measurements.

Results for ^{14}C at latitudes 70° and 9°N and 42°S are shown for the same months and years in Figures 4, 5, and 6 as were shown for 31°N in Figure 3. At 70°N, model results indicate better agreement in the stratosphere with Dynamics C than with either Dynamics A or B (see Figures 4*c* and 4*d*). The tropospheric results at 70°N are not quite as clear, although Dynamics B tends to transport more to the troposphere than is observed (see, e.g., dashed-dotted curve in Figure 4*b*). The model versus measurement results at 9°N show Dynamics A and B to be better representations than Dynamics C in the stratosphere in January 1964 and January 1966 (Figures 5*b* and 5*d*), whereas Dynamics C provides a better representation of ^{14}C in the stratosphere in January 1965 (Figure 5*c*). Generally, the tropospheric observations of ^{14}C at 9°N are better simulated with Dynamics C (see Figures 5*b*, 5*c*, and 5*d*). Carbon 14 in both the stratosphere and the troposphere is better represented at 42°S with Dynamics C than with either Dynamics A or B (see Figures 6*b*, 6*c*, and 6*d*).

Given the above discussion for latitudes 31°, 70°, 9°N and 42°S, we conclude that ^{14}C is best simulated with Dynamics C. The amount of ^{14}C in the stratosphere stays at levels more consistent with those that are measured. Dynamics C has a smaller ASTER than either Dynamics A or B (see discussion in section 2). Dynamics C also has a sharper transition in eddy diffusion coefficients (K_{yy} and K_{zz}) at the tropopause than do Dynamics A and B (see Table 2).

Kinnison [1989] found a better simulation of ^{14}C with a sharper transition in eddy diffusion at the tropopause. We ran a model sensitivity experiment in which Dynamics A was used with the sharper transition at the tropopause from Dynamics C. Carbon 14 was slightly better simulated in this modified Dynamics A simulation, but we conclude from this model experiment that the magnitude of the advective component of the strat/trop exchange rate is even more important than the severity of the eddy diffusion transition at the tropopause.

We also ran a model sensitivity experiment in which the eddy diffusion (both K_{yy} and K_{zz}) was taken from Dynamics C combined with the advective field from Dynamics A. This model experiment gave ^{14}C results that showed better agreement with measurements than those achieved with Dynamics A, but the agreement with measurements is not as good as that achieved with Dynamics C.

These results for ^{14}C imply that both advection and eddy

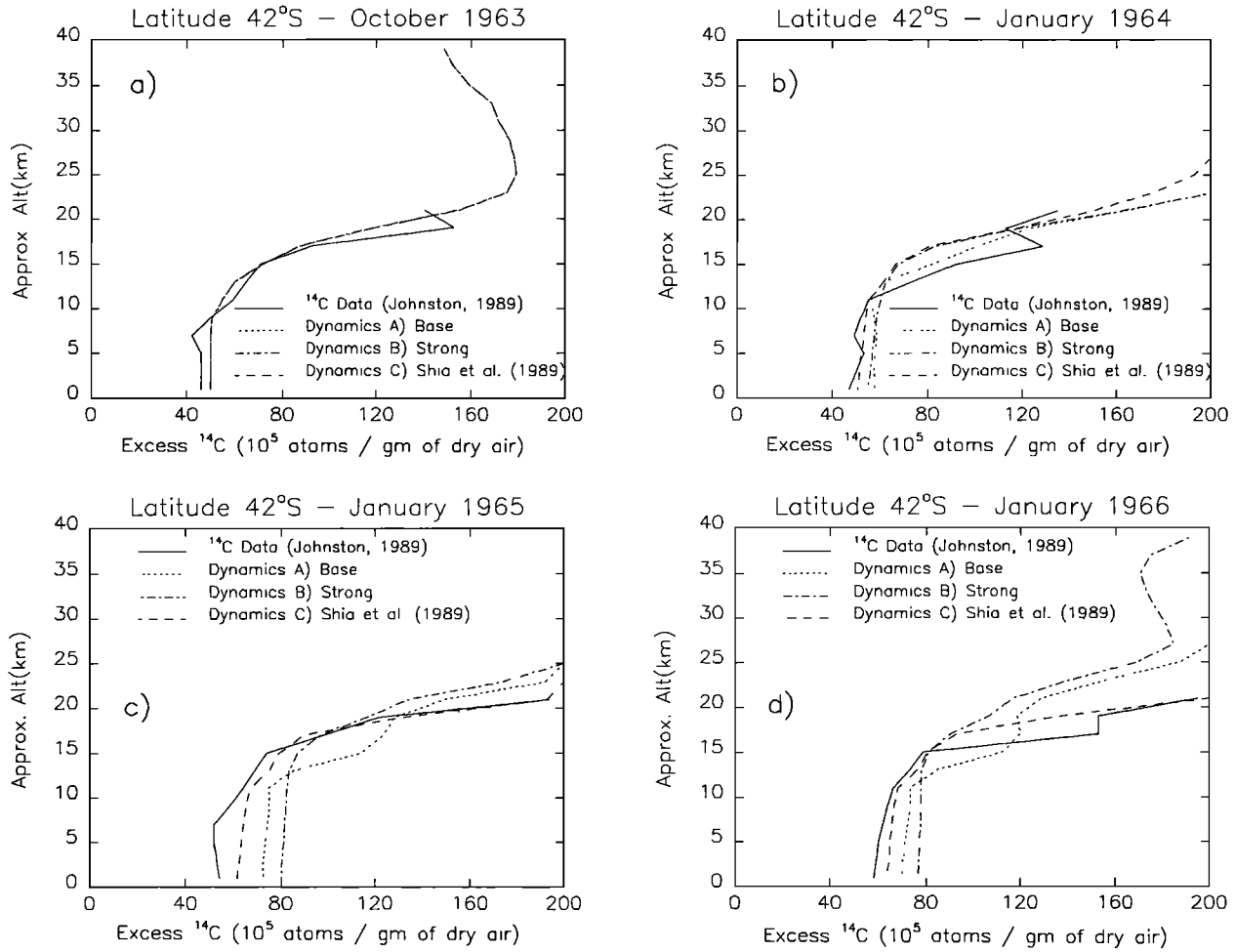

Fig. 6. Excess ^{14}C measurements and model simulations at 42°S at four different times: (*a*) October 1963, (*b*) January 1964, (*c*) January 1965, and (*d*) January 1966. Initial ^{14}C distribution in (*a*) for October 1963 (short dashed, dashed-dotted, and long dashed curves for the model simulations) is taken from *Johnston* [1989]. The solid curve represents the balloon data ((*a*), (*b*), (*c*), and (*d*)), while the short dashed, dashed-dotted, and long dashed curves represent the model simulation of ^{14}C for Dynamics A, B, and C, respectively, in (*b*), (*c*), and (*d*). The units are in 10^5 ^{14}C atoms per gram of dry air.

diffusion are important: (1) Advective transport between the stratosphere and troposphere is probably smaller than that computed by either Dynamics A or B and (2) eddy diffusion is probably more realistically represented in Dynamics C. These results are corroborated by the analysis of *Holton* [1990] which indicated mass fluxes through the 100 mbar surface of 1.3×10^{17} kg yr^{-1}. For Dynamics B the excess transport to the troposphere is clearly a result of the larger advective component of the strat/trop exchange rate (see section 2). The advective component of the strat/trop exchange rate is about 70% greater for Dynamics A than Dynamics C which will result in a larger flux of ^{14}C to the troposphere for Dynamics A. The eddy diffusion differences (mainly K_{yy}) between Dynamics A and C are also responsible for some of the disagreements in the model simulations. The K_{yy} in Dynamics C tend to move the ^{14}C equatorward (where upward motions predominate) and away from the larger downward vertical velocities at high latitudes, thus ^{14}C tends to be preserved longer in the stratosphere with Dynamics C.

6. Stratospheric Aircraft NO_x Injection Simulations

A fleet of commercial aircraft may someday fly in the stratosphere [*Douglass et al.*, 1991; *Johnston et al.*, 1991]. Possible effects on ozone have been investigated by several 2D models in preparation for a meeting (held in January 1991 at Virginia Beach, Virginia) to establish the ground work for new studies of stratospheric aircraft influence. Computations for seven scenarios of aircraft altitude and NO_x injection were undertaken. A fleet of 600 stratospheric flying planes were assumed to be flying at three different speeds and cruise altitudes.

A summary of the emission information about these stratospheric flying aircraft is given in Table 3. An emission index of 15 g of NO_x per kg of fuel used was assumed for all three scenarios ((*a*), (*f*), and (*g*)) discussed in this paper. Scenarios (*a*), (*f*), and (*g*) have Mach speeds of 2.4, 3.2, and 1.6, respectively. The difference among the three sce-

TABLE 3. Emission Information

Fuel Use, 70×10^9 kg yr^{-1}	
Speed and Cruise Altitude Mach 1.6, 14.3–17.4 km Mach 2.4, 16.8–19.8 km Mach 3.2, 21.3–24.4 km	
Latitude Band	Percent Used
Latitudinal Distribution of Fuel Use	
80°–90°N	0.6
70°–80°N	0.7
60°–70°N	0.7
50°–60°N	12.3
40°–50°N	28.4
30°–40°N	18.4
20°–30°N	8.4
10°–20°N	6.7
0°–10°N	6.3
0°–10°S	4.9
10°–20°S	4.2
20°–30°S	4.0
30°–40°S	3.1
40°–50°S	1.3
50°–90°S	0.0
Species	Value
Emission Indices, g/kg of Fuel	
NO_x	15
H_2O	1230
CO	1.5
CH_4	0.2

narios is in the cruise altitude; all other injection information is the same.

The lower boundary conditions for the transported constituents are given in Table 4. The source gases $C_2Cl_3F_3$, $C_2Cl_2F_4$, C_2ClF_5, $CHClF_2$, $CBrClF_2$, $CBrF_3$, and CH_3Br were added to the model. A baseline computation with no stratospheric aircraft was completed for each dynamical formulation before the scenarios of stratospheric aircraft were input. All model computations were for 20 years which gave a steady state annual condition. The baseline and perturbed steady state annual conditions were then compared with each other.

The total ozone change predicted for the three different dynamical formulations is given in Figure 7 for scenario (*a*). For Dynamics A (see Figure 7*a*), total ozone decreases larger than 2% are predicted for all latitudes north of 30°N and for the spring, summer, and early fall time period at 60°S. The total ozone decrease in Dynamics B (see Figure 7*b*) is much smaller with ozone decreases greater than 2% during about 9 months of the year but only at polar latitudes. Total ozone decrease with Dynamics C (see Figure 7*c*) is the largest with changes greater than 2% for all but a narrow region in the southern hemisphere tropics.

Total ozone change was also computed for two other scenarios, (*f*) and (*g*), for the three dynamical formulations. A yearly average global total ozone change was computed for all three scenarios and three dynamical formulations and is given in Table 5. We can summarize by stating that the smaller the advective component of the strat/trop exchange rate the larger the ozone depletion predicted by the model computation. Another way of stating this is: When the mass flow through this lower stratosphere is slow, the residence time of NO_x is longer, and therefore the level of the NO_x aircraft perturbation will be larger, leading to greater ozone loss.

7. Discussion and Conclusions

We have performed other sensitivity studies with these three dynamical formulations. Since 2D models in the past several years have been used to simulate the effect on stratospheric ozone in an environment of increasing Cl_x [e.g., *WMO*, 1990], we investigated the influence of these different dynamical formulations on a Cl_x perturbation. For these studies we increased Cl_x through the trace gases from 2.5 to 8.2 ppbv, CH_4 was doubled, and N_2O was increased by 20% (see Table 1). The yearly average global total ozone decrease for Dynamics A, B, and C was −2.4, −2.1, and −3.0%. When the advective component of the strat/trop exchange rate was small, a larger ozone decrease was computed.

The change in total ozone decrease from the different dynamical formulations is much less for a Cl_x perturbation (at least one resulting from source gas changes) than for a lower stratospheric NO_x injection. The ozone decrease from the Cl_x change ranges over about a factor of 1.4 for largest over smallest (−3.0/−2.1%, see above). The ozone decrease from the NO_x injection due to stratospheric aircraft varies from a factor of 8 (−1.2/−0.14%, see Table 5) for scenario (*f*) to a factor of 2.6 (−7.6/−4.1%, see Table 5) for scenario (*g*).

We have compared model predictions to other constituents of the atmosphere besides total ozone and ^{14}C. These comparisons included profile solar backscatter ultraviolet (SBUV) ozone data, limb infrared monitor of the stratosphere (LIMS) NO_2 and HNO_3 data, and stratospheric and mesospheric sounder (SAMS) N_2O and CH_4 data. These

TABLE 4. Lower Boundary Conditions for All Transported Species in Stratospheric Aircraft NO_x Injections

Species	Type of Boundary Condition, Units	2015 Value
N_2O	mixing ratio, ppbv	330
CH_4	mixing ratio, ppmv	2.05
CO	mixing ratio, ppbv	100
H_2	mixing ratio, ppbv	500
CH_3OOH	flux, cm^{-2} s^{-1}	0.0
CH_3Cl	mixing ratio, pptv	600
CH_3CCl_3	mixing ratio, pptv	150
CCl_4	mixing ratio, pptv	100
$CFCl_3$	mixing ratio, pptv	260
CF_2Cl_2	mixing ratio, pptv	510
$C_2Cl_3F_3$	mixing ratio, pptv	70
$C_2Cl_2F_4$	mixing ratio, pptv	10
C_2ClF_5	mixing ratio, pptv	8
$CHClF_2$	mixing ratio, pptv	200
O_x	deposition velocity, cm s^{-1}	0.1
HNO_3	mixing ratio, pptv	90
NO_y(wo HNO_3)	mixing ratio, pptv	10
Cl_x	flux, cm^{-2} s^{-1}	0.0
CH_3Br	mixing ratio, pptv	10
$CBrF_3$	mixing ratio, pptv	6
$CBrClF_2$	mixing ratio, pptv	2
Br_x	flux, cm^{-2} s^{-1}	0.0

Units are in parts per billion by volume (ppbv), parts per million by volume (ppmv), and parts per trillion by volume (pptv).

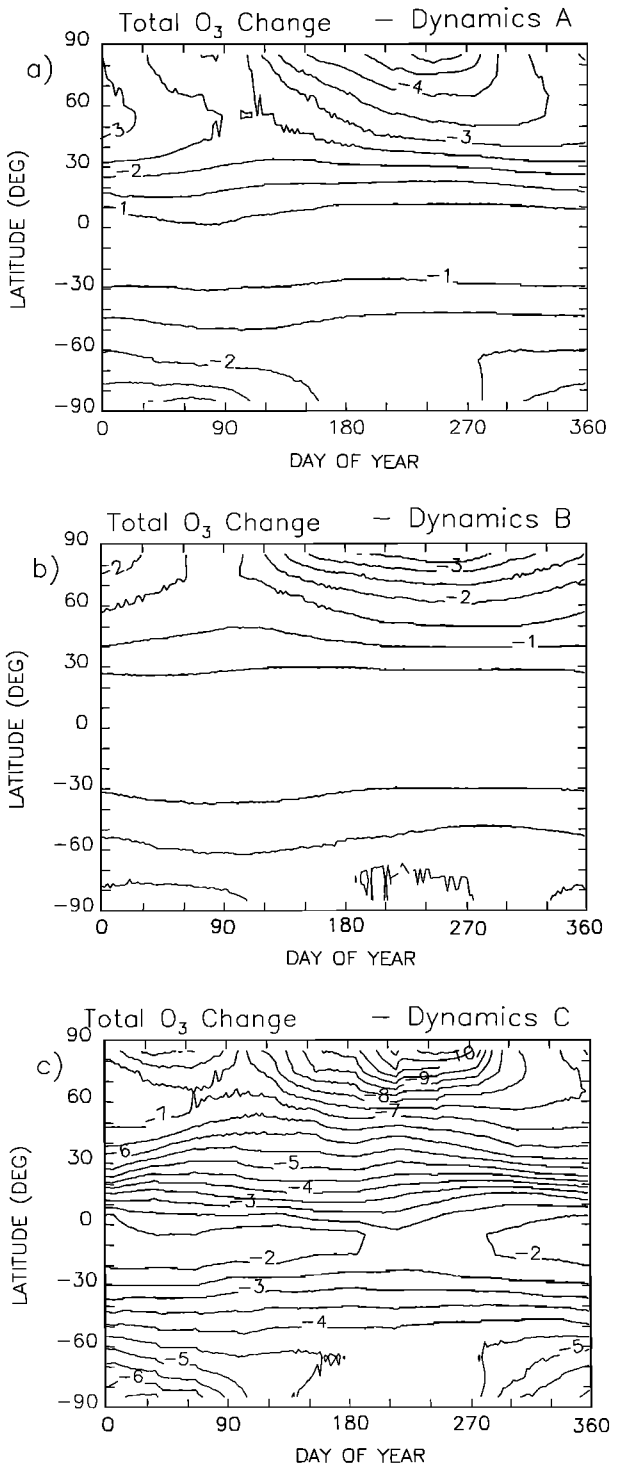

Fig. 7. Total percentage ozone change predicted from a model simulation for three scenarios using (*a*) Dynamics A, (*b*) Dynamics B, and (*c*) Dynamics C. Contour intervals are spacings of 0.5%.

model-measurement comparisons (with the exception of NO_2 and HNO_3 in the equatorial lower stratosphere) indicated that it would be difficult to differentiate between Dynamics A and C, if ^{14}C were not considered.

Equatorial lower stratospheric odd nitrogen (NO_y = N + NO + NO_2 + NO_3 + 2*N_2O_5 + HNO_3 + HO_2NO_2 + $ClONO_2$) constituents are generally underestimated from model simulations when compared with measurements unless a tropical odd nitrogen source like lightning is included [e.g., *Ko et al.*, 1986; *Jackman et al.*, 1987]. *Yang et al.* [1991], without including an NO_y lightning source, have noted a dramatic improvement in the model-measurement agreement of NO_y constituents with their new transport formulation. Since Dynamics C is based on an earlier version of the *Yang et al.* [1991] transport, it is no surprise that our simulations of NO_y constituents in the equatorial lower stratospheric are better with Dynamics C. For example, we present a model-measurement comparison for Dynamics A, B, and C compared to LIMS measurements of daytime NO_2 in Figure 8. This comparison is represented by showing the ratio of our model results to the LIMS values. Both the Dynamics A and B simulations show values less than 1.0 from 10 mbar down to 200 mbar, whereas the Dynamics C simulation indicates values closer to 1.0 above 50 mbar in the tropics and above 100 mbar in the middle to high latitudes.

TABLE 5. Global Total Ozone Change From NO_x Injections by Stratospheric Aircraft

Dynamics	O_3 Change From NO_x Injection by Aircraft, % Scenario*		
	(*a*)†	(*f*)‡	(*g*)§
A, base	−1.7	−4.1	−0.67
B, strong	−0.74	−2.9	−0.14
C, *Shia et al.* [1989]	−4.3	−7.6	−1.2

*H_2O is fixed in these model simulations.
†Scenario (*a*): Mach 2.4 (16.8–19.8 km), E.I. (emission index) (NO_x) = 15.
‡Scenario (*f*): Mach 3.2 (21.3–24.4 km), E.I. (NO_x) = 15.
§Scenario (*g*): Mach 1.6 (14.3–17.4 km), E.I. (NO_x) = 15.

If ^{14}C measurements are included in the analysis of which dynamics formulation is correct, Dynamics C with the small ASTER is thought to be the better representation of the transport in the stratosphere. Carbon 14 may not be a reliable tracer to use for model validations because (1) the ^{14}C data are suspect when compared to ^{90}Sr measurements taken at the same time [*Telegadas and List*, 1969] and contains a "hidden source" above 21 km [e.g., *Chang*, 1976] and (2) the temperature and derived transport in the 1963–1966 time period may be substantially different from that in the 1979–1983 time period (from which data are taken to compute the circulation used in our model simulations). To answer the first point, we note that *Johnston* [1989] has presented compelling arguments that ^{14}C measurements do indicate a hidden source of ^{14}C above 21 km and between 32° and 90°N in January 1963, but by October 1963 the ^{14}C at 31°N and above 24 km behaved about the same during the period 1960–1961 as it did during 1964–1965. The difference in shape between ^{14}C and ^{90}Sr in the October 1963 to December 1966 time period is thought to be due to the preferential attachment of ^{90}Sr on aerosols and therefore preferential settling of ^{90}Sr out of the lower stratosphere rather than by any hidden source of ^{14}C [*Johnston*, 1989]. With regard to the second point we note that we do not know if the stratospheric motion has changed substantially from 1963–1966 to 1979–1983 as there were no global measurements of the stratospheric temperature in the 1960s. If there are dramatic changes in the residual circulation from one year to another or even over longer time scales, then ^{14}C is not a very stringent test. If, on the other hand, the atmo-

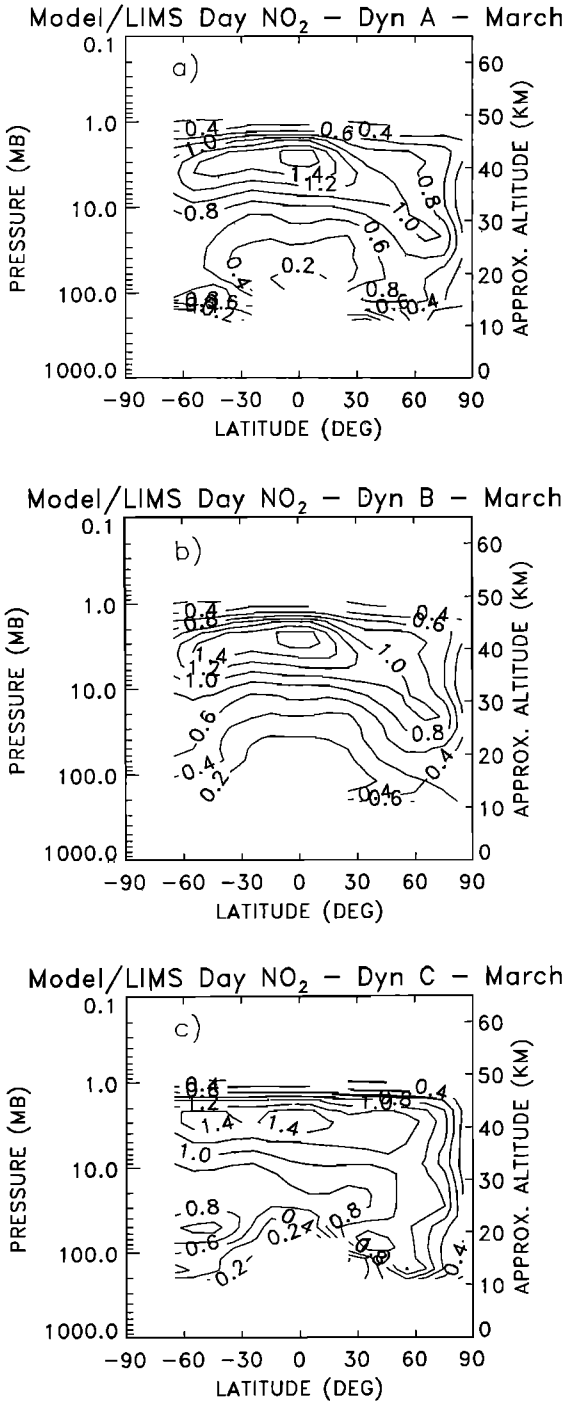

Fig. 8. Ratio of model simulated to LIMS measured daytime NO_2 using (*a*) Dynamics A, (*b*) Dynamics B, and (*c*) Dynamics C. Contour intervals are 0.2 apart.

sphere over time scales of decades shows relatively small excursions within a primarily sluggish lower stratosphere transport motion, then ^{14}C is a good test of model transport.

We find a very large sensitivity of total ozone to stratospheric aircraft NO_x injections. If the advective component of the strat/trop exchange rate is as small as indicated in the ^{14}C data and the eddy diffusion is more realistically represented by Dynamics C, as is also indicated in the ^{14}C data, then the model predictions of global total ozone change using Dynamics C will be the more reliable. If ^{14}C data is suspect and should not be used or if the modeled transport of the 1979–1983 time period cannot be applied to the 1963–1967 time period, then the model predictions of either Dynamics A or C are equally reliable, and the range of these two values gives a value of uncertainty for these model predictions; for example, our model predicts between a 1.7% (Dynamics A) and a 4.3% (Dynamics C) global total ozone change for scenario (*a*).

Dynamics B, with the largest ASTER, does not predict total ozone, ^{14}C, or any other species as well as either Dynamics A or C and should not be used to simulate stratospheric constituents. Even though Dynamics B has been found to be deficient in representing the stratosphere, the total ozone changes from simulations of stratospheric aircraft could be thought of as lower limits from our model computations which use only gas phase photochemical reactions. The global total ozone decrease from using Dynamics B for scenarios (*a*) and (*g*) are relatively small levels of less than 1%. The global total ozone decrease from using Dynamics B for scenario (*f*), flying at Mach 3.2 between 21.3 and 24.4 km, is a fairly large 2.9%.

This study has also been useful in validating deposition velocities ($\approx 6.7 \times 10^{-3}$ cm/s) and mean lifetimes ($\approx$6 years) for ^{14}C (and hence ^{12}C or CO_2) as well as pointing out the uncertainty in the dynamics of the lower stratosphere. More work is necessary to understand more thoroughly the advective component of the strat/trop exchange rate.

Finally, we note that none of our simulations included heterogeneous chemistry. *Weisenstein et al.* [1991] have indicated that heterogeneous chemistry can, in fact, change the sign of the ozone perturbation effect of stratospheric aircraft. They show that if the reaction

$$N_2O_5(\text{gas}) + H_2O(\text{aerosol}) \rightarrow 2\ HNO_3(\text{aerosol})$$

is included in simulations with an imposed sulfate aerosol layer, then stratospheric aircraft may increase ozone. This provocative result indicates that we still do not totally understand nor are we able to indisputably predict with present-day models the effects of stratospheric aircraft on ozone. More laboratory work and model simulations are necessary to help quantify the influence of these high-flying aircraft.

Acknowledgments. We thank Richard S. Stolarski (NASA Goddard Space Flight Center) for providing initial ^{14}C information and encouragement throughout this project. Yuk L. Yung (California Institute of Technology) kindly provided an early version of the Shia et al. (1989) paper for our use as well as a copy of the dynamics used in their ^{14}C simulations. Harold Johnston (University of California, Berkeley) is acknowledged for sending us an early version of the Johnston (1989) manuscript. We would like to thank Rita D. Rosen (Department of Energy/Environmental Measurements Laboratory) for providing us with several difficult to find Health and Safety Laboratory reports. One of us (SAK) was supported to work on this project during the summer of 1989 through the Summer Institute for Atmospheric Sciences which is sponsored by the Goddard Laboratory for Atmospheres. The authors acknowledge NASA Headquarters High Speed Research Program and the Atmospheric Chemistry Modeling and Analysis Program for support during the time that this project was undertaken. The authors thank two anonymous reviewers for constructive comments on this manuscript.

REFERENCES

Bhandari, N., D. Lal, and Rama, Stratospheric circulation studies based on natural and artificial radioactive tracer elements, *Tellus*, *18*, 391–405, 1966.

Chang, J., Uncertainties in the validation of parameterized transport in 1-D models of the stratosphere, Proceedings of the Fourth Conference of the Climatic Impact Assessment Program, edited by T. M. Hard and A. J. Broderick, *Rep. DOT-TSC-75-38*, 175–182, Dep. of Transp., Washington, D. C., 1976. (Available as *NTIS AD-A068982* from Natl. Tech. Inf. Serv., Springfield, VA).

DeMore, W. B., J. J. Margitan, M. J. Molina, R. T. Watson, D. M. Golden, R. F. Hampson, M. J. Kurylo, C. J. Howard, and A. R. Ravishankara, Chemical kinetics and photochemical data for use in stratospheric modeling, *JPL Publ. 87-41*, 196 pp., 1987.

Dopplick, T. G., The heat budget, in *The General Circulation of the Tropical Atmosphere and Interactions With Extratropical Latitudes*, vol. 2, edited by R. E. Newell, J. W. Kidson, D. G. Vincent, and C. J. Boer, pp. 27–94, MIT Press, Cambridge, Mass., 1974.

Dopplick, T. G., Radiative heating of the global atmosphere: Corrigendum, *J. Atmos. Sci.*, *36*, 1812–1817, 1979.

Douglass, A. R., C. H. Jackman, and R. S. Stolarski, Comparison of model results transporting the odd nitrogen family with results transporting separate odd nitrogen species, *J. Geophys. Res.*, *94*, 9862–9872, 1989.

Douglass, A. R., M. A. Carroll, W. B. DeMore, J. R. Holton, I. S. A. Isaksen, H. S. Johnston, and M. K. W. Ko, The Atmospheric effects of stratospheric aircraft: A current consensus, *NASA Ref. Publ. 1251*, 52 pp., 1991.

Dunkerton, T., On the mean meridional mass motions of the stratosphere and mesosphere, *J. Atmos. Sci.*, *35*, 2325–2333, 1978.

Garcia, R. R., and S. Solomon, A numerical model of the zonally averaged dynamical and chemical structure of the middle atmosphere, *J. Geophys. Res.*, *88*, 1379–1400, 1983.

Garcia, R. R., S. Solomon, R. G. Roble, and D. W. Rusch, A numerical response of the middle atmosphere to the 11-year solar cycle, *Planet. Space Sci.*, *32*, 411–423, 1984.

Gray, L. J., and J. A. Pyle, A two dimensional model of the quasi-biennial oscillation of ozone, *J. Atmos. Sci.*, *46*, 203–220, 1989.

Holton, J. R., On the global exchange of mass between the stratosphere and troposphere, *J. Atmos. Sci.*, *47*, 392–395, 1990.

Jackman, C. H., P. D. Guthrie, and J. A. Kaye, An intercomparison of nitrogen-containing species in Nimbus 7 LIMS and SAMS data, *J. Geophys. Res.*, *92*, 995–1008, 1987.

Jackman, C. H., P. A. Newman, P. D. Guthrie, and M. R. Schoeberl, Effect of computed horizontal diffusion coefficients on two-dimensional N_2O model distributions, *J. Geophys. Res.*, *93*, 5213–5219, 1988.

Jackman, C. H., A. R. Douglass, P. D. Guthrie, and R. S. Stolarski, The sensitivity of total ozone and ozone perturbation scenarios in a two-dimensional model due to dynamical inputs, *J. Geophys. Res.*, *94*, 9873–9887, 1989*a*.

Jackman, C. H., R. K. Seals, Jr., and M. J. Prather, Two-dimensional intercomparison of stratospheric models, *NASA Conf. Publ. 3042*, 608 pp., 1989*b*.

Jackman, C. H., A. R. Douglass, S. Chandra, R. S. Stolarski, J. E. Rosenfield, J. A. Kaye, and E. R. Nash, Impact of interannual variability (1979–1986) of transport and temperature on ozone as computed using a two-dimensional photochemical model, *J. Geophys. Res.*, *96*, 5073–5079, 1991.

Johnston, H. S., Evaluations of excess carbon 14 and strontium 90 data for suitability to test two-dimensional stratospheric models, *J. Geophys. Res.*, *94*, 18,485–18,493, 1989.

Johnston, H. S., D. Kattenhorn, and G. Whitten, Use of excess carbon 14 data to calibrate models of stratospheric ozone depletion by supersonic transports, *J. Geophys. Res.*, *81*, 368–380, 1976.

Johnston, H. S., M. J. Prather, and R. T. Watson, The atmospheric effects of stratospheric aircraft: A topical review, *NASA Ref. Publ. 1250*, 36 pp., 1991.

Kinnison, D. E., Effects of trace gases on global atmospheric chemical and physical processes, UCRL-53903, Ph.D. dissertation, Lawrence Livermore Natl. Lab., Univ. of Calif., Livermore, 1989.

Ko, M. K. W., N. D. Sze, M. Livshits, M. B. McElroy, and J. A. Pyle, The seasonal and latitudinal behavior of trace gases and O_3 as simulated by a two-dimensional model of the atmosphere, *J. Atmos. Sci.*, *41*, 2381–2408, 1984.

Ko, M. K. W., M. B. McElroy, D. K. Weisenstein, and N. D. Sze, Lightning: A possible source of stratospheric odd nitrogen, *J. Geophys. Res.*, *91*, 5395–5404, 1986.

Lal, D., and B. Peters, Cosmic ray produced radioactivity on earth, in *Encyclopedia of Physics*, edited by S. Flugge, vol. 46/2, pp. 551–612, Springer-Verlag, New York, 1967.

Legrand, M. R., F. Stordal, I. S. A. Isaksen, and B. Rognerud, A model study of the stratospheric budget of odd nitrogen, including effects of solar cycle variations, *Tellus*, *41*(B), 413–426, 1989.

Lingenfelter, R. E., and R. Ramaty, Astrophysical and geophysical variations in ^{14}C production, in *Radiocarbon Variations and Absolute Chronology*, edited by I. U. Olsson, pp. 513–537, Wiley Interscience, New York, 1970.

Liss, P. S., Tracers of air-sea gas exchange, *Philos. Trans. R. Soc. London, Ser. A*, *325*, 93–104, 1988.

List, R. J., and K. Telegadas, Using radioactive tracers to develop a model of the circulation of the stratosphere, *J. Atmos. Sci.*, *26*, 1128–1136, 1969.

McElroy, M. B., and R. J. Salawitch, Changing composition of the global stratosphere, *Science*, *243*, 763–770, 1989.

Newman, P. A., M. R. Schoeberl, R. A. Plumb, and J. E. Rosenfield, Mixing rates calculated from potential vorticity, *J. Geophys. Res.*, *93*, 5221–5240, 1988.

Oeschger, H., U. Siegenthaler, U. Schotterer, and A. Gugelmann, A box diffusion model to study the carbon dioxide exchange in nature, *Tellus*, *27*, 168–192, 1975.

Pyle, J. A., A calculation of the possible depletion of ozone by chlorofluorocarbons using a two-dimensional model, *Pure Appl. Geophys.*, *118*, 355–377, 1980.

Robinson, G. D., The transport of minor atmospheric constituents between the troposphere and the stratosphere, *Q. J. R. Meteorol. Soc.*, *106*, 227–253, 1980.

Rosenfield, J. E., M. R. Schoeberl, and M. A. Geller, A computation of the stratospheric diabatic residual circulation using an accurate radiative transfer model, *J. Atmos. Sci.*, *44*, 859–876, 1987.

Russell, J. M., III, S. Solomon, L. L. Gordley, E. E. Remsberg, and L. B. Callis, The variability of stratospheric and mesospheric NO_2 in the polar winter night observed by LIMS, *J. Geophys. Res.*, *89*, 7267–7275, 1984.

Shia, R. L., Y. L. Yung, M. Allen, R. W. Zurek, and D. Crisp, Sensitivity study of advection and diffusion coefficients in a two-dimensional stratospheric model using excess carbon 14 data, *J. Geophys. Res.*, *94*, 18,467–18,484, 1989.

Stordal, R., I. S. A. Isaksen, and K. Horntveth, A diabatic circulation two-dimensional model with photochemistry: Simulations of ozone and long-lived tracers with surface sources, *J. Geophys. Res.*, *90*, 5757–5776, 1985.

Tans, P. A., Computation of bomb C-14 data for use in global carbon model calculations, in Carbon Cycle Modelling, edited by B. Bolin, *SCOPE 16*, 131–157, 1981.

Tans, P. P., I. Y. Fung, and T. Takahashi, Observational constraints on the global atmospheric CO_2 budget, *Science*, *247*, 1431–1438, 1990.

Telegadas, K., Seasonal stratospheric distribution of cadmium-109, plutonium-238, and strontium-90, *Rep. HASL-184*, pp. I53–I118, U.S. At. Energ. Comm., Clearinghouse, Dep. of Comm., Springfield, Va., 1968.

Telegadas, K., The seasonal atmospheric distribution and inventories of excess carbon 14 from March 1955 to July 1969, *USAEC Rep. HASL-243*, pp. I-2–I-87, U.S. At. Energ. Comm., Health and Safety Lab., New York, 1971.

Telegadas, K., and R. J. List, Are particulate radioactive tracers indicative of stratospheric motions?, *J. Geophys. Res.*, *74*, 1339–1350, 1969.

Tung, K. K., and H. Yang, Dynamical component of seasonal and year-to-year changes in Antarctic and global ozone, *J. Geophys. Res.*, *93*, 12,537–12,559, 1988.

Warneck, P., *Chemistry of the Natural Atmosphere*, International Geophysics Series, edited by R. Dmowska and J. R. Holton, vol. 41, Academic, San Diego, Calif., 1988.

Watson, R. T., M. J. Prather, and M. J. Kurylo, Present state of knowledge of the upper atmosphere 1988: An assessment report, *NASA Ref. Publ. 1208*, 208 pp., 1988.

Wei, M.-Y., D. R. Johnson, and R. D. Townsend, Seasonal distri-

butions of diabatic heating during the first GARP global experiment, *Tellus*, *35*(A), 241–255, 1983.

Weisenstein, D., M. K. W. Ko, J. M. Rodriguez, and N. D. Sze, Impact of heterogeneous chemistry on model-calculated ozone change due to HSCT aircraft, *Geophys. Res. Lett.*, *18*, 1991–1994, 1991.

Widhopf, G. F., L. Glatt, and E. Ruth, Two-dimensional description of potential perturbations to the ozone layer due to NO_x and H_2O aircraft emissions, *FAA-EE-84-11*, Fed. Aviat. Admin., 1984.

World Meteorological Organization (WMO), Atmospheric ozone: 1985, *WMO Rep. 16*, Washington, D. C., 1986.

World Meteorological Organization (WMO), Report of the international ozone trends panel: 1988, *WMO Rep. 18*, Washington, D. C., 1988.

World Meteorological Organization (WMO), Scientific assessment of stratospheric ozone: 1989, *WMO Rep. 20*, Washington, D. C., 1990.

Yang, H., K. K. Tung, and E. Olaguer, Nongeostrophic theory of zonally averaged circulation, II, Eliassen-Palm flux divergence and isentropic mixing coefficient, *J. Atmos. Sci.*, *47*, 215–241, 1990.

Yang, H., E. Olaguer, and K. K. Tung, Simulation of the present-day atmospheric ozone, odd nitrogen, chlorine and other species using a coupled 2-D model in isentropic coordinates, *J. Atmos. Sci.*, *48*, 442–471, 1991.

K. F. Brueske, Research and Data Systems Corporation, 7855 Walker Drive, Suite 460, Greenbelt, MD 20770.

A. R. Douglass and C. H. Jackman, Laboratory for Atmospheres, NASA Goddard Space Flight Center, Mail Code 916, Greenbelt, MD 20771.

S. A. Klein, Department of Atmospheric Science, University of Washington, Seattle, WA 98195.

(Received April 16, 1991;
revised September 30, 1991;
accepted September 30, 1991.)